C. Cheng,[1] *Ph.D.; T. E. Kirkbride,*[1] *B.Sc.; D. N. Batchelder,*[1] *Ph.D.; R. J. Lacey,*[2] *Ph.D.; and T. G. Sheldon,*[2] *B.Sc.*

In Situ Detection and Identification of Trace Explosives by Raman Microscopy

REFERENCE: Cheng, C., Kirkbride, T. E., Batchelder, D. N., Lacey, R. J., and Sheldon, T. G., "**In Situ Detection and Identification of Trace Explosives by Raman Microscopy,**" *Journal of Forensic Sciences,* JFSCA, Vol. 40, No. 1, January 1995, pp. 31–37.

ABSTRACT: The innovative design of the newly developed Renishaw Raman Microscope system and its application to the in situ detection and identification of plastic explosives contained in fingerprint samples are presented. Raman microscopy is a nondestructive inspection method. Our experimental results show that Raman spectra and Raman band images can be obtained from explosive particles as small as 1 μm^3 in size or 1 picogram in mass. After exploring the full potential of the Raman microscopic technique, the aim of this research is to develop a real-time and field-deployable plastic explosive detection system.

KEYWORDS: forensic science, criminalistics, Raman microscopy, plastic explosive, fingerprint examination

Raman spectroscopy is a well established technique for analyzing and identifying materials. The idea of using it to characterize explosives was first suggested in 1964 [*1*]. Conventional Raman instruments have, however, suffered from poor light throughput and low efficiency so that experimental work has been confined to laboratory darkrooms. In-field applications could not be considered under these conditions. The poor light throughput was caused by extensive use of gratings, mirrors and lenses required by the instruments mainly for eliminating the strong Rayleigh scattered light which comes together with the Raman scattered light. Furthermore the photomultipliers common in the traditional Raman systems have relatively low quantum efficiency and need to be carefully protected from over exposure. For these reasons, Raman instruments tended to be heavy and expensive, were difficult to align and required highly skilled operators. To overcome these difficulties and to widen the field of applications, many spectroscopists have been working to modernize Raman instrumentation. Small and robust Raman spectrometers capable of working in a non-laboratory environment are now available.

Development of a compact Raman microprobe/microscope system was started by the Leeds University group in the late 1980s [*2*]. Prototype units were developed and successfully tested before commercialized units were manufactured by Renishaw plc. [*3,4*]. In the Police Scientific Development Branch, research work on explosive traces detection can be traced back to the early 1980s. The objective of the Raman project is to produce a highly sensitive and nondestructive technique to investigate fingerprint samples that may contain traces of explosives; a brief report summarizing the early Raman work has been presented [*5*]. In this paper, we describe the Renishaw Raman microscope system design and report on the experimental work on the detection of plastic explosives, in particular their traces in the fingerprint samples.

Received for publication 22 April 1994; revised manuscript received 16 June 1994; accepted for publication 17 June 1994.

[1] The Department of Physics, The University of Leeds, Leeds, England.

[2] Police Scientific Development Branch, St. Albans, Hertfordshire, England.

The Samples

SEMTEX-H was used as the source of explosive material for this study. This explosive has two active chemical ingredients: Cyclotrimethylene-trinitramine or RDX and Pentaerythritol-tetranitrate or PETN. RDX and PETN are present in the explosive as transparent micrometer size crystals bound together by an amorphous waxy material. The structural formulae of RDX and PETN are shown in Fig. 1. The crystal structures of the two materials were determined by X-ray diffraction some twenty years ago [*6,7*]. Raman spectra of RDX and PETN were first reported by Hodges and Akhavan [*8,9*] who used Fourier Transform Raman (FTR) spectroscopy; recently very similar results were obtained by McNesby et al. [*10*] with the same technique.

Transfer of trace explosives from the source to the surface of a substrate by means of finger contact and hence producing the fingerprints in a depletion series has been reported by Neudorfl et al. [*11*]. We have tested a variety of materials, such as wood, glass and cardboard, as the substrate but found that a flat metal surface is the most suitable. Hence the results presented here are mainly from fingerprint samples made on aluminum sheet. In a depletion series the same fingertip which has been contaminated with explosive has been used repeatedly to leave prints on 4×4 cm^2 aluminum sheets. Forty sheets are used in each depletion series, the explosive residue decreasing with the increasing number. The exact quantity of the explosive in a fingerprint has not been determined but we believe it ranges from micrograms down to nanograms. To simulate real life conditions we also made "impure" samples with fingertips which were cross contaminated by both SEMTEX and other greasy substances.

Techniques other than Raman microscopy are available for analyzing the explosive materials but they require removing samples from the fingerprints; the disadvantages from the forensic science point of view are obvious. In contrast the Raman technique is nondestructive. With the Renishaw Raman Microscope system, the study has been made *in situ.* The samples were simply placed onto the microscope sample stage for either visible light observation or for full spectral measurements; no further sample prepara-

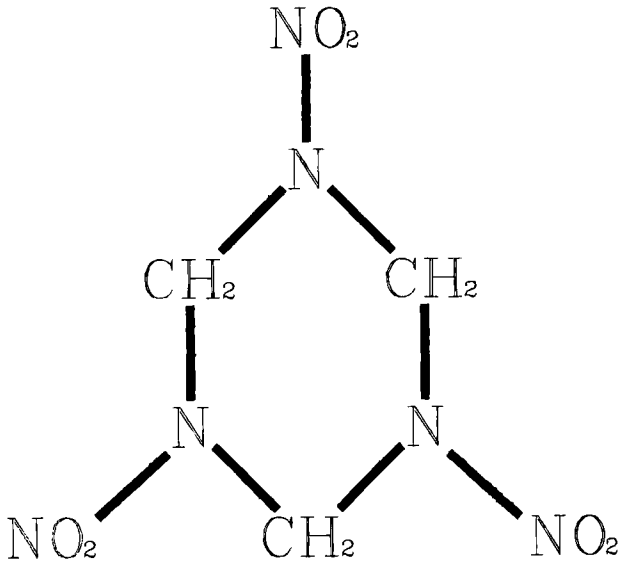

(RDX)

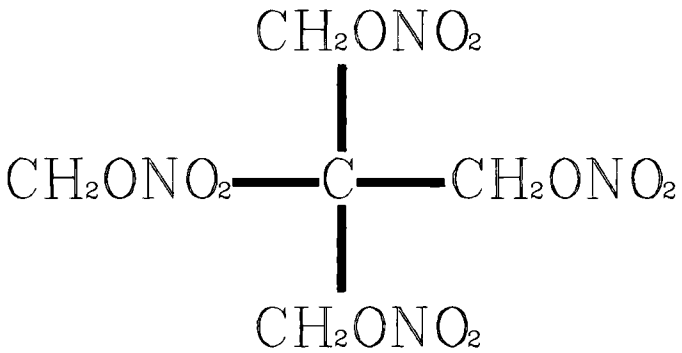

(PETN)

FIG. 1—*Chemical structures of RDX and PETN.*

tion was needed. The fingerprints were not destroyed by the measurement and could be re-examined later either by Raman or other methods.

Raman Microscopy and the Instrument

Raman scattering is a weak effect that is usually observed by focusing a laser beam upon a sample. The scattered light is collected by lenses and directed into a spectrometer to determine the frequencies or wavelengths. The major component of the scattered light, called Rayleigh scattered light, has the frequency of the incident laser and therefore can not be used to characterize the chemical compositions of the samples. Raman scattered light, a small portion of the total, appears at lower frequencies (only the Stokes lines are concerned in this application). The change of the frequency is caused by the interaction between the incident laser beam (the photons) and the molecular vibrational modes (the phonons). Each of these vibrational modes is characterized by a certain energy or frequency; if this mode is Raman active then a peak will appear in the spectrum. The frequency difference between this peak and the laser line is called the Raman shift. A given molecule will give a characteristic Raman spectrum with several peaks; bigger and more complex molecules tend to give more Raman peaks. The intensities of the Raman peaks reflect the concentration of the molecules within the sample. The whole spectrum also contains information about the structure of the molecule and its environment.

Rayleigh scattering is very much weaker than the incident laser beam and Raman scattering is even weaker, with typical orders of magnitude as follows:

$$I_{(ex)} > 10^3 \times I_{(ray)} > 10^8 \times I_{(ram)}$$

here $I_{(ex)}$, $I_{(ray)}$ and $I_{(ram)}$ are the light intensities of the exciting laser beam, the Rayleigh scattered light and the Raman scattered light, respectively. Hence it is essential that the spectrometer has a sensitive detector and that the Rayleigh light is efficiently rejected for good Raman spectra to be obtained.

Work on Raman microscopy began in the 1970s [*12*]. The basic idea is to use a high numerical aperture microscope objective as the lens to focus the laser beam and to collect the scattered light. The focal spot and/or the size of the sample is on the order of one to a few microns. Its success in examining miniature samples has made the technique popular, so that most commercial Raman instruments now have an optical microscope as an attachment. Figure 2 shows schematically the layout of the Renishaw Raman Microscope. It has been designed to perform two functions: the microprobe, which takes Raman spectra from micron size samples, and the microscope, which produces 2D magnified images using only the Raman scattered light. The Raman spectrum is used to identify the particle of explosive while the Raman image highlights their spatial distribution.

The Renishaw system, as is shown in Figure 2, consists of a spectrometer on the right hand side and an optical microscope on the left. The instrument employs two holographic notch filters (HNF) [*13*], the first functioning as the combination of a beamsplitter and a rejection filter and the second purely as a rejection filter. Depending upon its fine angle tuning, one HNF is able to reject the light at the laser frequency to the order of 10^{-5} to 10^{-6} and still transmit more than 80% of the light at other frequencies. In the instrument the laser beam is directed onto the sample by the mirrors, the beam collimator (two lenses), the first HNF and the microscope objective. The 180° back scattered light from the sample is collected by the same objective and fed back into the spectrometer. The Rayleigh scattered light and reflected light are blocked by the two HNFs but the Raman scattered light is transmitted. The combined result of the two HNFs, at best, reduces the intensities of Rayleigh scattered light by a factor of 10^{-12}. This high rejection rate allows the use of only a single grating stage in the spectrometer even with highly scattering samples. Optics in the system are designed in conjunction with the microscope; this coupled with the use of the HNFs has improved the light throughput dramatically.

When taking a Raman image the laser beam is defocused through

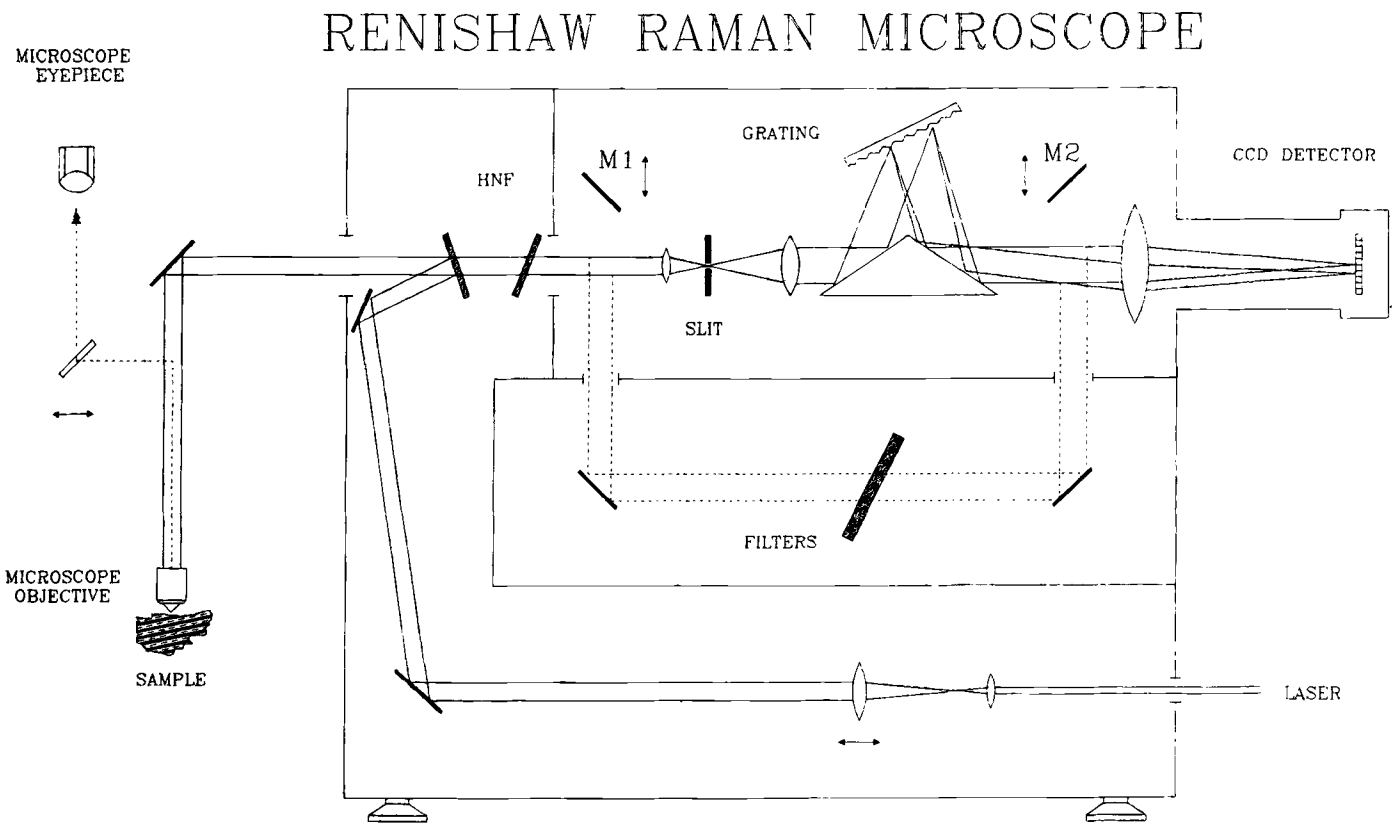

FIG. 2—*Schematic diagram of the Renishaw Raman microscope.*

the adjustment of the beam collimator to illuminate an area of the sample. Scattered light from this area is collected to form the image. Two movable mirrors, M_1 and M_2 allow the instrument to perform the Raman microprobe function when set at the "out" positions. At the "in" positions, the beam of the scattered light is deflected by the mirrors to bypass the grating stage and go through the imaging filter; the instrument is then functioning as the Raman microscope. The filter stage holds a group of five or six dielectric narrow-band-pass filters, each of which has a different transmission band. The center of the filter transmission band is a function of the incident angle of the light, so that effectively each filter can be tuned to cover a spectral range of several hundred wavenumbers. The whole Raman spectrum is covered by the group of filters. This novel way of making 2D Raman band images with the tunable dielectric filters is also many times more efficient than conventional scanning methods.

The instrument covers the spectral range from 100 cm^{-1} to 4000 cm^{-1} (or more than that in special cases). Spectral resolution in the microprobe mode is 1 cm^{-1} and in the microscope mode, 20 cm^{-1}. The Raman imaging field is presently limited to a region of 300 μm (with ×10 objective) in diameter but in principle it is possible to image a larger area. Spatial resolution of the imaging mode, or the minimum size of the laser focus spot of the spectral mode, is 1 μm.

Improvements of instrument performance are also due to the employment of the CCD detector and modern personal computer. The CCD detector, a two dimensional electronic photographic plate, has a high quantum efficiency and very low dark current. It, and all the other moving stages in the instrument, are cable-linked with a PC and controlled by the operator through the keyboard. Data acquisition is fast and straightforward. Taking advantage of the 2D sensor, a new method with no pinhole aperture has been developed for performing confocal Raman spectroscopy. The spectra can be obtained from a small and well defined sample volume which is 1 μm in diameter and 2 μm in depth [*4*]. This technique can be used, for example, to determine the phase structures inside a bulk sample [*14*].

As the result of the high light throughput, compact lasers with a moderate power output of 25 mW are commonly used as the light sources of the Renishaw Raman Microscope. The whole instrument, including a laser and a computer, can be placed onto a table with area less than 2 square meters. The instrument is robust, relatively easy to transport and re-align; it does not require special laboratory facilities. Routine work can even be performed on a simple desk or table in the presence of daylight or room light. A trained technician can move the instrument to a new location and set it up in working order within a few hours. Only basic knowledge on how to use optical microscopes, lasers and PCs is required.

Results and Discussion

Typical Raman spectra from RDX and PETN crystals, several microns on a side, deposited on a silicon wafer are shown in Fig. 3, *a*) is for RDX and *b*) for PETN. The measurements were made with a 25 mW HeNe laser emitting at 632.8 nm. A X20, NA = 0.45, microscope objective was used. The amount of power reaching the sample was about 5 mW, which corresponds to an energy density of 2×10^9 W/m^2. Acquisition time for the above two spectra was 5 s. Both RDX and PETN appear to have large Raman scattering cross sections, making the Raman spectra easy to acquire. We have also tested a 514.5 nm line Ar+ laser with the same samples

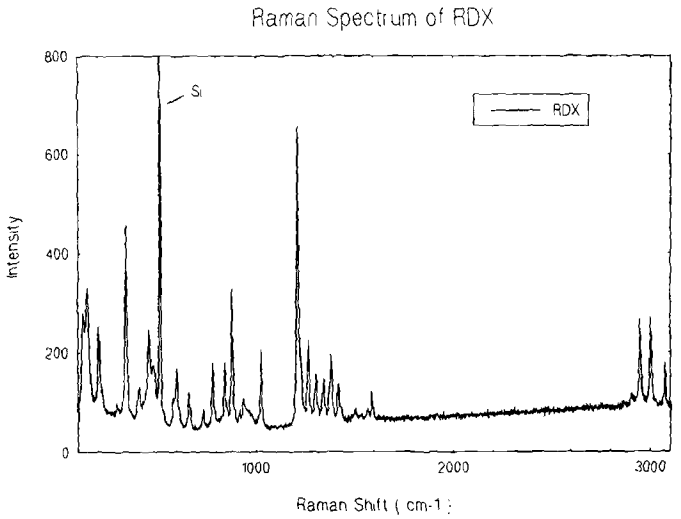

FIG. 3*a*—*Raman spectra of micron sized RDX and PETN samples (on a silicon wafer).*

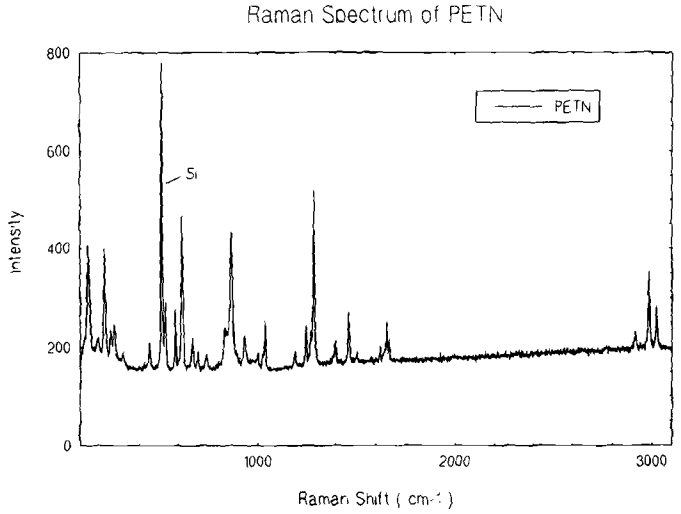

FIG. 3*b*—*PETN.*

and obtained essentially identical results. The spectra are similar in appearance to those acquired at lower spectral resolution using the FT Raman technique with much greater laser powers and longer recording times [*9,10*].

The intention of this paper is to demonstrate that a plastic explosive like SEMTEX can be identified by simply taking a Raman spectrum or a Raman band image. Table 1 is a list of all the Raman bands appearing in the spectra shown by Fig. 3. The relative peak intensities are shown by letter indexes: S means strong, M moderate and W weak; the V prefix means very. P indicates the peak is polarized. On first inspection the Raman spectra from different RDX particles often look somewhat different because most of the particles are individual single crystals. For a single crystal sample, the intensities of the polarized Raman bands depend upon the angle differences between the polarization plane of the laser and the crystalline orientation. The frequencies remain the same, however.

Polarized Raman spectra taken from a RDX single crystal are shown in Fig. 4. The crystal was grown in our laboratory and came out rectangular in shape, approximately $1 \times 2 \times 5$ mm^3 in size. We defined the X, Y and Z axes accordingly; therefore the

TABLE 1—*List of the Raman bands of RDX and PETN.*

RDX	(CM^{-1})	PETN	(CM^{-1})
129	S		
152	S	147	S
		194	W
207	S		
226	W	229	S
		260	M
		280	M
304	VW		
		321	W
345	VS, P		
413	M		
463	S	458	M
487	M		
		539	MS
589	W	589	MS
606	M		
		625	VS
668	M	677	M
		705	M
737	W		
		751	W
787	M		
849	M	840	M
		874	VS
885	S		
922	W		
944	W	941	M
		1005	VW
1031	S, P	1033	VW
		1045	M
		1195	W
1217	VS, P		
1235	M, P		
		1253	M
1272	S, P	1279	M
		1294	VS
1312	S, P		
1350	M, P		
1390	M, P		
		1405	W
1426	M, P		
		1471	M
1509	VW	1512	VW
1573	VW		
1595	W, P		
		1631	VW
		1662	M
		1675	M
2909	W	2917	W
2953	M		
		2990	M
3006	M		
		3024	M
3079	M		

longest dimension of the crystal was along Z and the two flat surfaces in the YZ planes. Theoretical analysis shows that the intensity of Raman scattered light is proportional to the square of the dipole moment induced in the sample by the incident radiation. This dipole moment u is written as:

$$u = aE \tag{1}$$

or

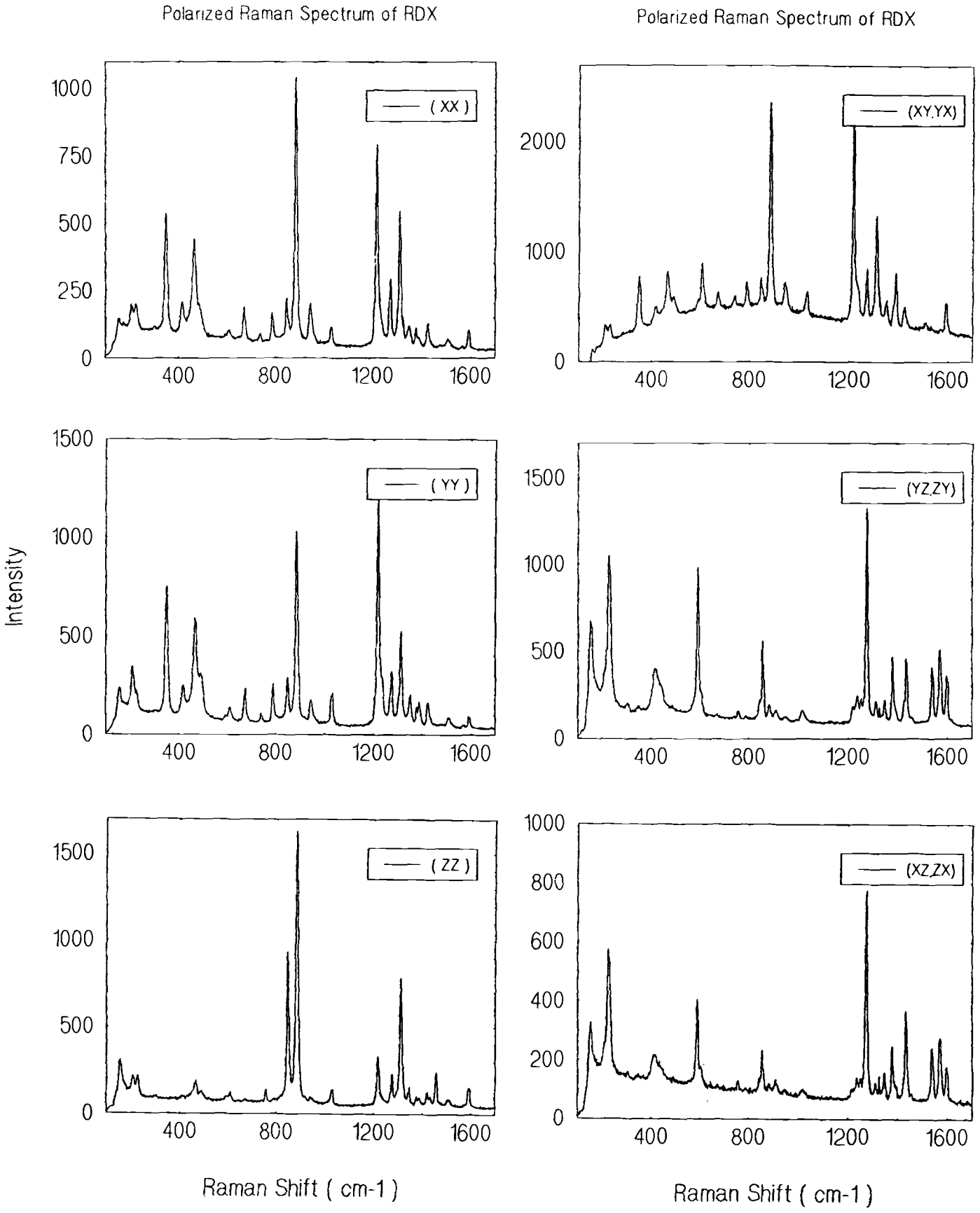

FIG. 4—*Polarized Raman spectra of a large RDX crystal.*

$$u_x = a_{xx}E_x + a_{xy}E_y + a_{xz}E_z$$
$$u_y = a_{yx}E_x + a_{yy}E_y + a_{yz}E_z \quad (2)$$
$$u_z = a_{zx}E_x + a_{zy}E_y + a_{zz}E_z$$

where E is the electric field of the incident laser beam and a the polarizability tensor. By orienting the RDX crystal sample with the microscope sample stage and arranging a polarization analyzer in front of the spectrometer, nine Raman spectra were obtained. Each of these spectra reflects the contribution from one of the nine elements of the polarizability tensor, such as, XX, YY, ZZ, XY, YX, XZ, ZX, YZ or ZY etc. Only the six independent spectra are shown here because of the fact that $a_{xy} = a_{yx}$, $a_{xz} = a_{zx}$ and $a_{yz} = a_{zy}$. In addition to proving that the RDX particles are single crystals, this type of study provides detailed information about the symmetries of the vibrational modes.

Spectral information for the pure RDX and PETN samples provides the foundation for the Raman imaging work on SEMTEX. Raman images are normally taken at one or two selected Raman bands which are intense and distinguishable from the background. RDX has a strong band at 885 cm^{-1} and PETN a strong band at 874 cm^{-1}, neither of which are polarization dependent. The 20 cm^{-1} wide imaging filter window can be centered at 880 cm^{-1} to cover both. A typical imaging result is shown in Fig. 5. The two micrographs were taken from the same area of an explosive contaminated fingerprint sample; on the left is the visible light image and on the right the Raman band image. A ×50 objective was used for this measurement. The fluorescence background was subtracted from the Raman image using the computer software. It can be seen from the photographs that the visible light image shows all particles, SEMTEX, dust and grease, etc., but the background-free Raman image shows only the RDX and PETN particles.

As previously described, the action of CCD camera is controlled by the PC. When the instrument is in the imaging mode, repeat exposures can be taken and the images will be read out and shown on the PC monitor. It is easy to acquire the visible light images in real time but the Raman images take considerably longer as the intensity of the Raman scattered light is weak. Hence an integration time is needed to build up a screen contrast on the PC monitor. The exposure time for taking the Raman image shown in Fig. 5 was 10 minutes. This long exposure time is not always necessary, especially in the case where Raman imaging is used to select certain targets for the spectral analysis and therefore the image background does not matter very much. A 20 s exposure Raman band image without background subtraction is shown in Fig. 6. This Raman image is of an area in the 40th fingerprint sample from the depletion series; alongside is the visible light image from the same area. If, under certain conditions, less contrast is tolerable, the image can even be produced with only a few seconds exposure. However, for making a positive judgment, the background-free Raman images are more reliable.

The applicability of the Raman imaging detection technique has been further tested by a series of experiments on "impure" samples. Those samples often exhibit a strong fluorescence background which is sometimes considerably more intense than the Raman scattered light. It has been found that very fluorescent "dust" particles may appear in a Raman band image. For those samples we always deploy the microprobe afterwards to examine the reliability of the Raman image. Figure 7 shows spectra taken from the object of dimensions 5 μm^3 visible in the Raman image of Fig. 5. The figure shows the series of spectra taken with different exposure time: 1 s, 5 s, 10 s, 20 s and 40 s, respectively. The insert is the 1 s spectrum shown in an enlarged intensity scale. These spectra confirm that the particle is RDX. In the same way, Fig. 8 shows Raman spectra from a 1 μm^3 particle observed in the Raman image of Fig. 5. The spectra confirm that the particle of approximately 1 picogram mass is PETN. The particle was

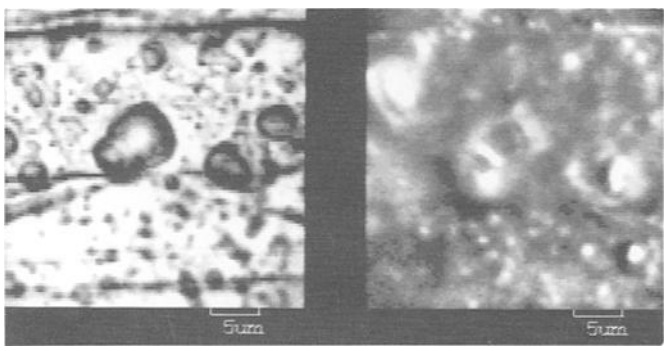

FIG. 5—*Images of a SEMTEX fingerprint sample:* a) *visible light image;* b) *background-subtracted Raman image.*

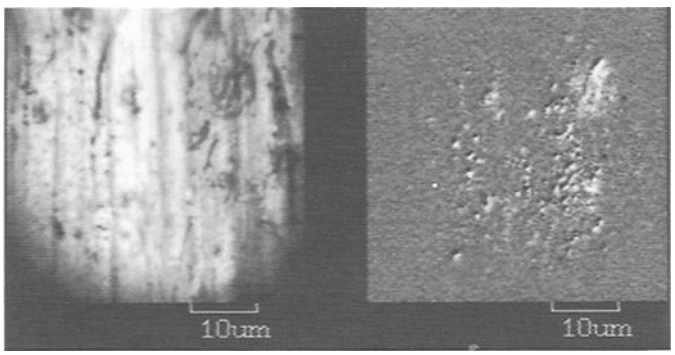

FIG. 6—*Images of the 40th fingerprint sample in a depletion series:* a) *visible light image;* b) *Raman band image with 20 s exposure time.*

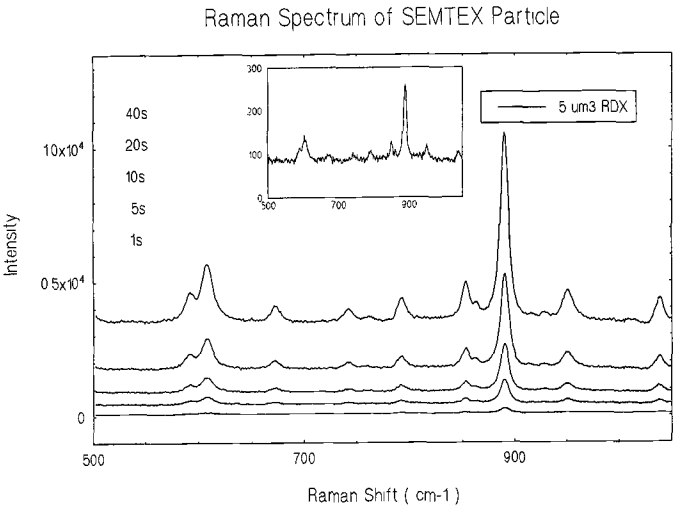

FIG. 7—*Raman spectra of a 5 μm^3 size particle (RDX): from the bottom to the top, 1 s, 5 s, 10 s, 20 s and 40 s exposures, respectively. The insert shows the 1 s data with a magnified intensity scale.*

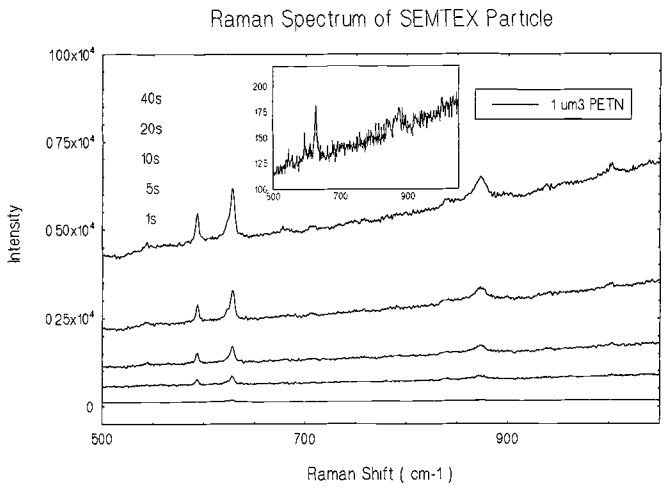

FIG. 8—*Raman spectra of a 1 μm³ size particle (PETN): from the bottom to the top, 1 s, 5 s, 10 s, 20 s and 40 s exposures, respectively. The insert shows the 1 s data with a magnified intensity scale.*

surrounded by the binding wax which caused the high background signal. Our experimental results indicate that for the impure samples, 1) Raman imaging can filter out the majority of the nonexplosive particles; 2) all the explosive particles tend to show up clearly in the Raman image; 3) acquiring spectral confirmation is simple and quick. The confidence level of Raman imaging detection is high, though false alarms can not be totally ruled out. Further checking of suspect particles by taking a full Raman spectrum is necessary for confirmation.

Conclusion

We have presented experimental results showing that the detection and identification of plastic explosive traces by means of Raman microscopy is not only feasible but practical. It has also been confirmed that examination of fingerprint samples can be performed *in situ* and over short time scales. The Raman microscopic technique is highly specific and capable of identifying explosive samples 1 μm^3 in volume or 1 picogram in mass quantity. The imaging analysis has a high confidence rate with further spectral analysis capable of providing confirmation.

Acknowledgment

We acknowledge the contributions Dr. I. P. Hayward, from the Department of Physics, the University of Leeds, has made to the Raman project and thank him for his helpful comments on the draft manuscript.

References

[1] Urbanski, T., *Chemistry and Technology of Explosives,* Vol. I, PWN Polish Scientific Publishers, Warszawa, 1964.

[2] Batchelder, D. N., Cheng, C., Muller, W., and Smith, B. J. E., "A Compact Raman Microprobe/Microscope: Analysis of Polydiacetylene Langmuir-Blodgett Films," *Die Makromolekulare Chemie Macromolecular Symposia,* Vol. 46, 1991, pp. 171–179.

[3] Batchelder, D. N., "Renishaw Transducer Systems Ltd. and The University of Leeds—Collaboration Leads to a New Image," *Measurement Science and Technology,* Vol. 3, No. 3, 1992, pp. 561–563.

[4] Williams, K. P. J., Pitt, G. D., Batchelder, D. N., and Kip, B., J., "Confocal Raman Microspectroscopy Using a Stigmatic Spectrograph and CCD Detector," *Applied Spectroscopy,* Vol. 48, No. 2, 1994, pp. 232–235.

[5] Batchelder, D. N. Cheng, C., Hayward, I. P., Lacey, R. J., Pitt, G. D., and Sheldon, T. G., "Raman Microscopy and 2-D Direct Imaging of Explosives and Drugs," *The Proceedings of Contraband & Cargo Inspection Technology,* Washington, DC, Oct. 1992, pp. 73–75.

[6] Choi, C. S. and Prince, E., "The Crystal Structure of Cyclotrimethylene-trinitramine," *Acta Crystallographica,* B28, 1972, pp. 2857–2862.

[7] Cady, H. H. and Laeson, A. C., "Pentaerythritol Tetranitrate II: Its Crystal Structure and Transformation to PETN I; an Algorithm for Refinement of Crystal Structures with Poor Data," *Acta Crystallographica,* B31, 1975, pp. 1864–1869.

[8] Hodges, C. M. and Akhavan, J., "The Use of Fourier Transform Raman Spectroscopy in the Forensic Identification of Illicit Drugs and Explosives," *Spectrochimica Acta,* Vol. 46A, No. 2, 1990, pp. 303–307.

[9] Akhavan, J., "Analysis of High-Explosive Samples by Fourier Transform Raman Spectroscopy," *Spectrochimica Acta,* Vol. 47A, No. 9/10, 1991, pp. 1247–1250.

[10] McNesby, K. L., Wolfe, J. E., Morris, J. B., and Pesce-Rodriguez, R. A., "Fourier Transform Raman Spectroscopy of Some Energetic Materials and Propellant Formulations," *Journal of Raman Spectroscopy,* Vol. 25, 1994, pp. 75–87.

[11] Neudorfl, P., McCooeye, M. A., and Elias, L., "Testing Protocol for Surface: Sampling Detectors," *The Proceedings of the 4th International Symposium on the Analysis and Detection of Explosives,* Jerusalem, Sept., 1992, pp. 337–343.

[12] Rosasco, G. J., Etz, E. S., and Cassatt, W. A., "The Analysis of Discrete Fine Particles by Raman Spectroscopy," *Applied Spectroscopy,* Vol. 29, No. 5, 1975, pp. 396–404.

[13] Yang, B., Morris, M. D., and Owen, H., "Holographic Notch Filter for Low-Wavenumber Stokes and Anti-Stokes Raman Spectroscopy," *Applied Spectroscopy,* Vol 45, No. 9, 1991, pp. 1533–1536.

[14] Garton, A. G., Batchelder, D. N., and Cheng, C., "Raman Microscopy of Polymer Blends," *Applied Spectroscopy,* Vol. 47, No. 7, 1993, pp. 922–927.

Address requests for reprints or additional information to
C. Cheng, Ph.D.
Department of Physics
University of Leeds
Leeds, England LS2 9JT